Compact spectrophotometer using polarization-independent liquid crystal tunable optical filters

Elena Nicolescu and Michael J. Escuti

North Carolina State Univ, Dept Electrical & Computer Engineering, Raleigh, NC (USA)

ABSTRACT

We introduce and demonstrate a simple spectrophotometer system insensitive to input polarization and with strong potential for compact and low-cost implementation. This technology has a wide variety of potential applications ranging from astronomy to medicine and even the cosmetics industry. To enable more powerful and portable microspectrometers we employ a novel design based on a tunable liquid crystal filter with polarization-independence, which is constructed of stacked liquid crystal polarization gratings (LCPGs). These switchable, anisotropic, thin diffraction gratings exhibit unique properties that include diffraction at visible and infrared wavelengths that can be coupled between only the zero- and first-orders (with nearly 100% and 0% experimentally verified efficiencies), depending on the applied voltage and wavelength of incident light. When combined with an elemental spatial filter, polarization-independent bandpass tuning can be achieved with minimum loss. Analogous to Lyot and Solc filters, several LCPGs are layered and introduced into a temporally resolved system using a single photodetector. The unique filter design enables improvement in terms of resolution and sensitivity by eliminating the polarization dependence present in all competing birefringence-based technologies. Also, the temporal detection system has a potential for improved miniaturization compared to any competing relevant approach and decreased cost by avoiding highly sensitive alignment, reflective diffraction components, Fabry-Perot cavities, and expensive detectors. In this work we describe the core principles of the tunable filter, present a representative spectrometer system design, report preliminary experimental data, and discuss the capabilities of the system in terms of spectral range, resolution, and sensitivity.

Keywords: spectrophotometer, spectrometry, polarization gratings, tunable optical filter, liquid crystals

1. INTRODUCTION

The applications of modern spectroscopy technologies include astronomy, medicine, education, remote-sensing, and even cosmetics. Although these applications are very diverse, they share a common dependency on technological advances in the field of spectroscopy, especially in terms of cost and portability. In recent years, consistent efforts have aimed to miniaturize the traditional laboratory spectrometer and decrease its cost. Unfortunately, these improvements required a significant decrease in functionality, especially in terms of resolution and sensitivity.

In an effort to improve cost and portability while minimizing the sacrifice in performance, we present a spectrometer design concept which (i) is based on liquid crystal polarization gratings (LCPGs), (ii) is polarization-independent, (iii) uses a temporal detection system with a single photodetector, and (iv) has a potential for increased signal sensitivity, and decreased cost and size since polarizers, dispersive gratings, and CCD arrays are not used. Fig. 1 shows the basic design of the system, with three essential elements: a stacked assembly of LCPGs, an elemental spatial-filter (or its equivalent), and a photo-detector.

In this work, we describe, demonstrate and analyze this portable spectrometer system. We examine its performance in terms of its essential properties including spectral resolution, sensitivity and spectral range. We also compare to currently available products and evaluate its potential for maximizing portability and efficiency while minimizing cost.

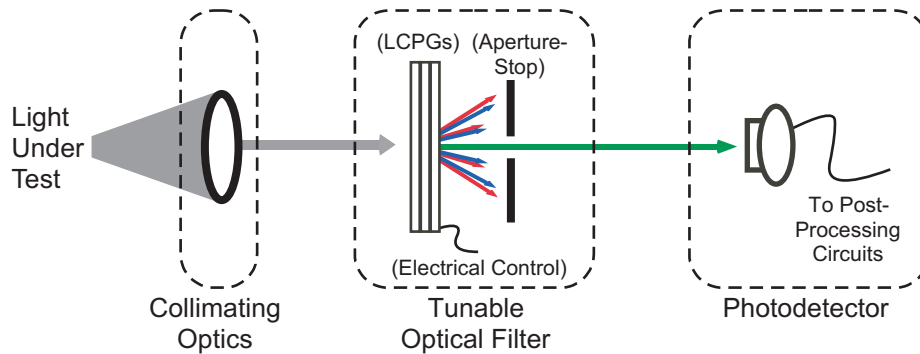Correspondence should be addressed to: mjescuti@ncsu.edu, +1 919 513 7363

Figure 1. Basic structure of the LCPG polarization independent tunable optical filter spectrometer design. (color figure)

2. BACKGROUND

2.1 Previous Work

Various compact spectrophotometer designs have been demonstrated including the Czerny-Turner,[1,2] Fabry-Perot,[3,4] Lyot-type[5,6] and even MEMs[2] based configurations. The Czerny-Turner configuration is one of the more common designs for spectrophotometers. The principle of this design uses a diffraction grating to separate the wavelengths which are then detected using a CCD array. The main disadvantage of this design is that it is dependent on spatial dispersion thereby causing decreased resolution with increased minituarization.

Tunable Fabry-Perot etalon filters have also been used in portable spectroscopy. These are composed of two highly reflective mirrors separated by a distance which, along with the refractive index of the material between the plates, determines the finesse of the filter. The cavity may be filled with nematic liquid crystal which allows the filter to be tuned by applying voltage instead of changing the distance between the plates.[7] Although this design boasts a wide free spectral range and tunable range, high resolution, and low driving voltage, its main disadvantage is that it requires the use of polarizers in order to pass the extraordinary (tunable) mode of light and block the ordinary (non-tunable) mode. A reduced polarization dependence has also been achieved by the addition of birefringent quarter waveplates[4] in an optical fiber-based scheme.

Optical bandpass/notch filters have also been implemented using stacked birefringent layers. Traditional Lyot-Ohman,[5,8] Solc[9–11], and Evans[12] filters are composed of a series of birefringent plates and polarizers. In order to achieve electrical tunability, the traditional birefringent plates can be replaced with a series of variable liquid crystal waveplates.[13] The primary disadvantage of such systems is their dependence on polarizers, which significantly increases signal loss and which are difficult/costly to implement at wavelengths outside the visible range.

2.2 Mathematical Basis for Temporally Resolved Spectrophotometer

Regardless of the type of tunable bandpass/notch filter used in a temporally-scanning spectrophotometer, the same principle of operation applies. We therefore begin by deriving the generic algorithm of our system, and subsequently apply it to our novel LCPG tunable optical filters. Fig. 1 illustrates the generic design of a spectrophotometer based on a scanned bandpass filter and a single photodetector. Given an input intensity spectrum $f(\lambda)$, a passband filter centered at λ_0 with a transfer function $h(\lambda - \lambda_0)$ and a photodetector responsivity $R(\lambda)$, then the detector photocurrent can be generically written as

$$I_p(\lambda_0) = \int_{\lambda_{min}}^{\lambda_{max}} f(\lambda)R(\lambda)h(\lambda - \lambda_0)d\lambda \qquad (1)$$

where λ_{min} and λ_{max} are the limits of the incident wavelength range. In many cases, it may be possible to consider the responsivity as that of a simple linear photodetector:[14]

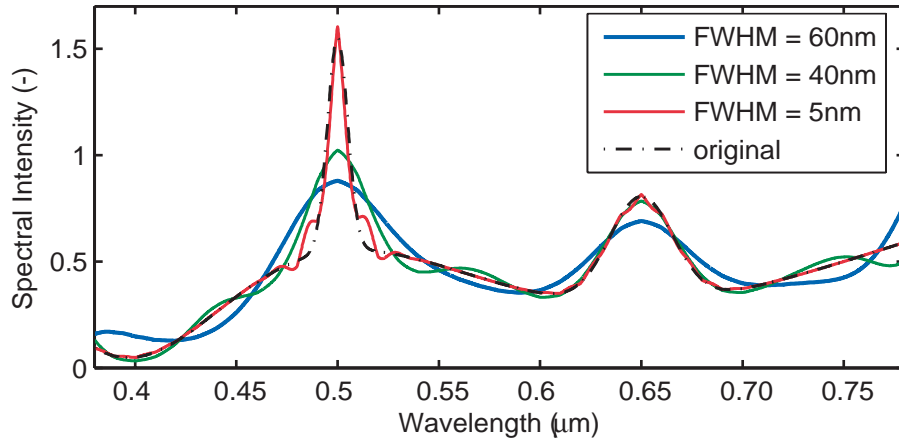$$R(\lambda) = \frac{\eta q \lambda}{hc} \qquad (2)$$

Figure 2. Calculated examples of spectra reconstruction for various values of FWHM. A Gaussian function is assumed for the kernel (the ideal filter function). (color figure)

where η is the quantum efficiency of the photodetector, q is the charge of an electron, h is Planck's constant, and c is the vacuum speed of light.

If we ensure that the input spectrum is zero outside of λ_{min} and λ_{max}, then Eq. (1) can be expressed as a convolution,

$$I_p(\lambda_0) = \big(g(\lambda) * h(\lambda)\big)(\lambda_0) = \int_\infty^\infty g(\lambda)h(\lambda - \lambda_0)d\lambda, \tag{3}$$

where $g(\lambda) = f(\lambda)R(\lambda)$. Keep in mind that $h(\lambda - \lambda_0)$ is known *a priori*, $I_p(\lambda_0)$ is measured, and we seek a solution for $f(\lambda)$. Since this can be posed as a convolution-deconvolution problem, it is therefore convenient to proceed in the Fourier domain (since this convolution becomes a multiplication), where k is the frequency:

$$\widetilde{I}_p(k) = \widetilde{g}(k)\widetilde{h}(k) \tag{4}$$

We can now solve for $\widetilde{g}(k)$, perform the Fourier inverse transform, and re-normalize by the responsivity. The original spectrum therefore results:

$$f(\lambda) = \mathcal{F}^{-1}\left\{\frac{\widetilde{I}_p(k)}{\widetilde{H}(k)}\right\}\frac{1}{R(\lambda)}. \tag{5}$$

Note that this basic deconvolution approach may in some cases need to be replaced by methods that are more robust to measurement noise (e.g. Wiener deconvolution, among others).

The basic principle of detection can now be summarized: a tunable bandpass filter is scanned while a photocurrent is measured, and the original input spectrum can be reconstructed through Fourier transforms and knowledge of the detector responsivity. While Eq. (5) is useful for analytic work, it must be implemented numerically for actual computation in a spectrometer system.

For convenience in this preliminary work, we describe our passband filter $h(\lambda - \lambda_0)$ as being proportional to a Gaussian function with mean λ_0 and variance $\sigma^2 = FWHM^2/8\ln 2$, where $FWHM$ corresponds to the full-width at half-maximum of the passband:

$$h(\lambda - \lambda_0) = \exp\left(\frac{-4\ln 2(\lambda - \lambda_0)^2}{FWHM^2}\right) \tag{6}$$

We acknowledge that the actual shape of our LCPG filter is a product of $\cos(...)^2$ terms (see Section 3), but we assume that the Gaussian is a good first-order approximation.
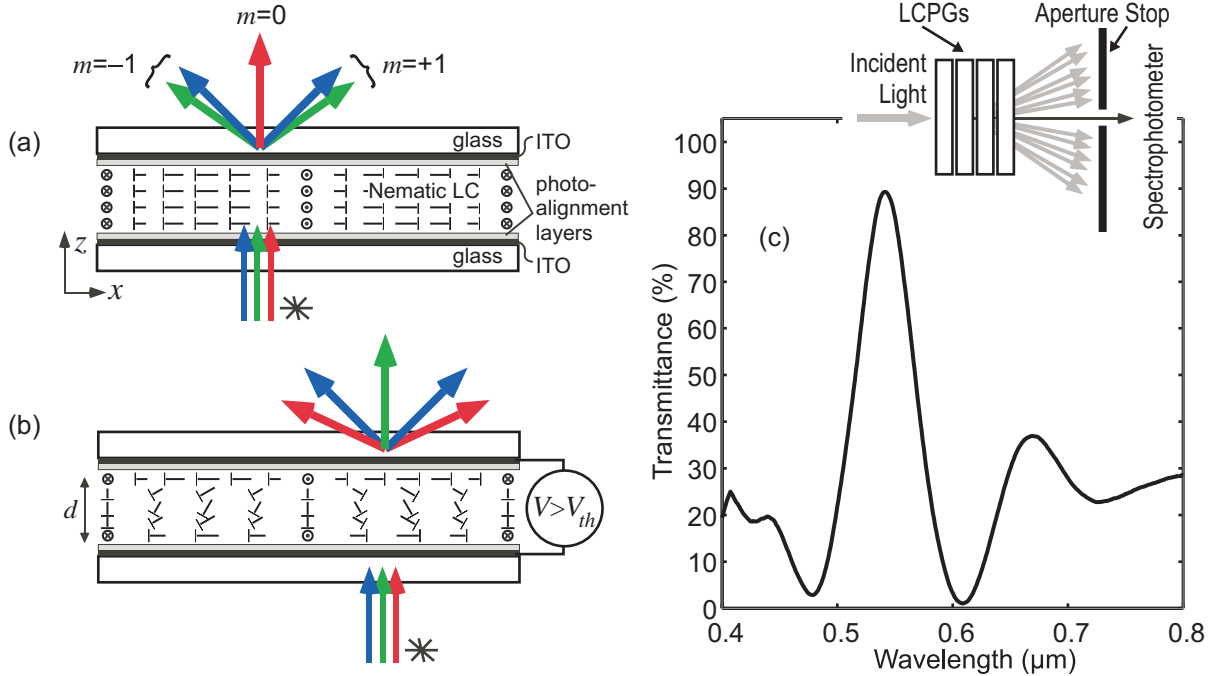
Figure 3. The principle of operation of the LCPG tunable optical filter: (a) Basic geometry (side view) and illustrated diffraction behavior when $\Delta nd=$ red wavelength with zero applied voltage - note that only the ±1-orders are ideally present regardless of input polarization; (b) Diffraction behavior when the applied voltage exceeds V_{th} - note that light at different wavelengths couple into the zero-order; (c) total spectrum of the four laminated stages (optically coupled with glue)

It is evident that in reconstructing a signal that has been filtered by a Gaussian passband such as the one described above, the FWHM plays an important role. Understandably, the more a filter resembles an impulse function (i.e. $FWHM$ is as small as possible), the more accurate and resolved the signal reconstruction will be. Fig. 2 shows the calculated reconstruction of an example input signal after being processed with a Gaussian filter function with varied $FWHM$. Clearly, a minimum $FWHM$ is desired for accurate reconstruction, but a $FWHM$ of up to 60nm is sufficient to minimally detect a spectral feature on the order of 20 nm. With this in mind, we now introduce the polarization-independent optical filter based on a recently developed switchable diffractive optical element.

3. LCPG TUNABLE OPTICAL FILTERS

The basic component of our novel optical filter[15] is the Liquid Crystal Polarization Grating. This is a switchable, anisotropic, diffraction grating actively being developed for many applications, including high-efficiency microdisplays,[16, 17] hyperspectral polarimetry,[18] and generic diffractive optical elements[19–22] . In another paper at this same conference,[15] we show how they can be configured to achieve a compelling polarization-independent tunable optical filter.

Polarization gratings[23, 24] (PGs), sometimes called anisotropic or vectorial gratings, are embodied as a spatially varying birefringence and/or dichroism, which in this case is a continuous, in-plane, linear birefringence texture[23–25] with a uniaxial optical anisotropy that follows the spatial profile $\mathbf{n}(x) = [\sin(\pi x/\Lambda), \cos(\pi x/\Lambda), 0]$, where Λ is the grating period. An effective way[16, 19, 26] to create this is using bulk nematic LCs aligned by photo-alignment surfaces that have been exposed with a polarization hologram, leading to the structure illustrated in Fig. 3(a) and (b) where the linear birefringence Δn is embodied in a nematic director $\mathbf{n}(x)$. Several notable properties of PGs are most relevant:[15, 18] (i) the zero-order can theoretically vary from 100% to 0% depending on the retardation $\Delta nd/\lambda$; (ii) the specular transmitted intensity is independent of input polarization and Λ;

and (*iii*) peak zero-order efficiencies occur at wavelength $\lambda_N = \Delta nd/N$, where N is a non-negative integer corresponding to the spectral fringe.

Electrical control of the diffraction efficiency occurs by decreasing the effective birefringence. As an external voltage V is applied (Fig. 3(b)), the nematic director reversibly reorients out-of-plane, thereby leading to a blue-shift in the entire spectrum.[15] As an illustrated example, if the product Δnd is set so that red light is transmitted when $V = 0$ and lower wavelengths are predominantly diffracted (Fig. 3(a)), then a small applied voltage $V > V_{th}$ could transmit green light and predominantly diffract red and blue (Fig. 3(b)). Note that even when d is large, the voltage threshold can be designed to remain approximately 1-2 V.

The concept of using stacked LCPGs as an optical filter is relatively simple, and is illustrated in the inset of Fig. 3(c). We stack three or more LCPGs of potentially different thicknesses and block all but the zero-order using a spatial filter of some kind. The transmittance of the LCPG stack is therefore a multiplication of the individual zero-order efficiencies and the losses due to Fresnel reflections and electrode absorption:

$$T(\lambda) = K^M \prod_{m=1}^{M} \eta_{0,m}(\lambda) = K^M \prod_{m=1}^{M} \cos^2 \left(\frac{\pi \Delta nd_m}{\lambda} \right) \qquad (7)$$

where M is the total number of stages, K is the combined transmittance of the substrates and electrodes within each stage, $\eta_{0,m}(\lambda)$ is the efficiency of stage m, and d_m is the LC layer thickness of grating m. Keep in mind that it is most accurate to consider $\Delta n \to \Delta n(V)$, which accomplishes the tuning effect. Given a design wavelength λ_0 and LC material, the relation $d = N\lambda_N/\Delta n$ can be employed to determine a minimum thickness required by setting $N = 1$. Note that the thinnest LCPG must be at least thick enough to exhibit one full-wave retardation ($\Delta nd_1 \geq \lambda_0$).

There are several design possibilities[15] involving the choice of d_m and M, which have their impact on the primary bandpass filter parameters. For our initial experimental work here, we constructed a four-stage LCPG tunable optical filter with a compound progression[15] ($M = 4$). We utilized a nematic LC MLC-6080 (Merck, $\Delta n = 0.202$ at 589 nm) and chose a design wavelength $\lambda_0 = 0.56 \mu m$. Fabrication details are contained in Ref.[15] We chose to use nominal thicknesses of $d_1 = 3$ μm (one wave retardation), $d_2 = 6$ μm (two wave retardation), and $d_3 = d_4 = 9$ μm (three wave retardation). The transmission spectra of the LCPG tunable filter that results when we laminate the four stages together is shown in Fig. 3(c). As predicted, a bandpass filter notch appears at $\lambda_0 = 0.56$ μm, with high peak transmittance ($\sim 88\%$), substantially higher than almost any tunable optical filter approach using polarizers. We also observe a minimum FWHM (57 nm) close to that predicted (68 nm) by analyzing Eq. (7). The electrical tuning characteristics of this LCPG optical filter are shown in Fig. 4. The voltage-resolved spectra are shown in 4(a), where we notice that the notch persists even over a modest tuning range (540 nm to 480 nm is $\sim 10\%$ of the starting wavelength), and that low voltages (< 2.2 V) are needed. The central wavelength of the bandpass peak and the FWHM for each tuning voltage are shown in Fig. 4(b).

Note that this particular filter represents only our initial trials in implementing the LCPG optical filter. Based on our simulations (as seen from the FWHM and finesse graphs in Ref.[15]), there is much room for improvement via filter design (more and thicker stages) and fabrication process optimization. Nevertheless, we utilize this four-stage LCPG optical filter to evaluate our proposed spectrophotometer.

4. SPECTROMETER DESIGN AND IMPLEMENTATION

A key feature of our spectrometer design is its relative simplicity. It does not require the use of polarizers, bulky lens systems, or complex drive electronics. Fig. 5 shows a schematic of the spectrophotometer system. The input to the system is a collimated light beam, composed of the spectra to be measured, directly incident on the LCPG tunable filter stack. At the output of the filter stack, a simple aperture stop is utilized to block all but the 0-order beam. Alternatively, a spatial filter, a total-internal-reflection (TIR) prism, or a multimode fiber collimator could be used to couple the zero-order light to the photodetector while blocking the rest.

The tunable optical filter is controlled by a voltage divider circuit used to set the proper voltage ratios between the individual cells to ensure a desirable filter profile. An amplitude-modulated 4 kHz signal is applied typically at a modulating frequency around 2 Hz and with a triangular envelope profile. The resulting periodic photodetector signal can then be easily post-processed with maximum speed and accuracy.
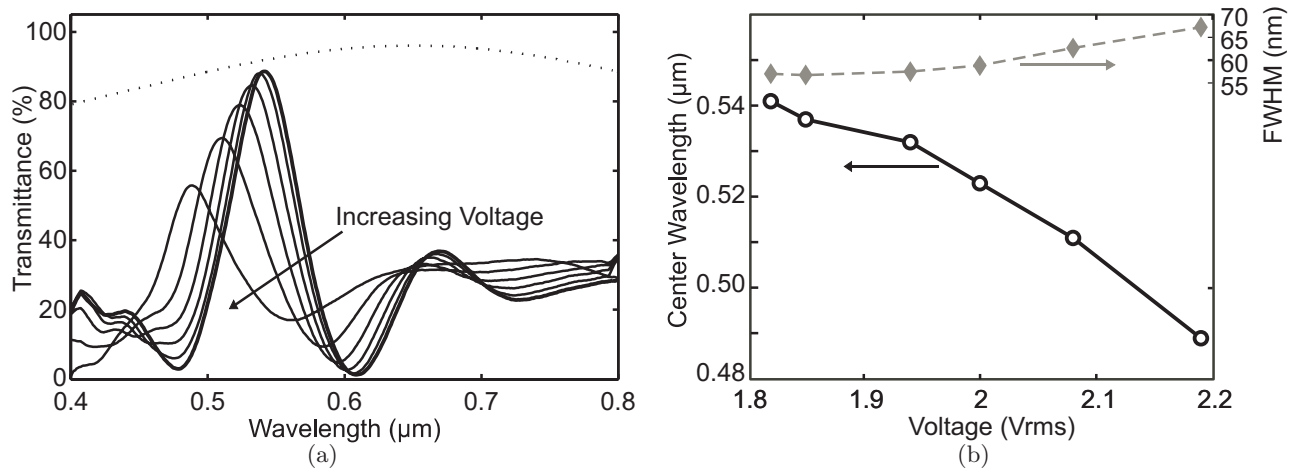
Figure 4. Electrical tuning characteristics of a four-stage LCPG optical filter: (a) Transmission spectra for various voltages (1.82 V, 1.85 V, 1.94 V, 2.00 V, 2.08 V, and 2.19 V); and (b) Voltage response of the bandpass center wavelength and FWHM. Note that the dotted line in part (a) is a reference spectra including the substrate absorption and interface losses, obtained as an assembly of four stages filled only with glue.
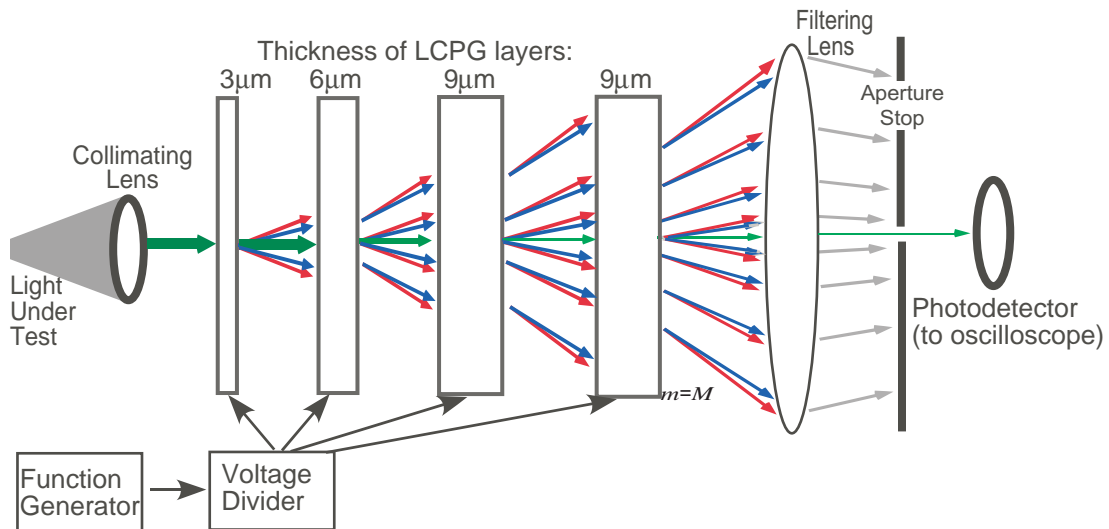

Figure 5. Detailed structure of the full spectrometer system. (color figure)

5. PRELIMINARY RESULTS

As a proof-of-principle, we measured a small portion of the spectrum of a commercial shortpass filter (Edmund Industrial Optics NT47-285) illuminated by an incandescent lamp (Fig. 6(a)). The filter has a very narrow peak at 0.502 μm which we do not expect to be able to fully resolve with the preliminary LCPG filter employed – nevertheless the challenge is instructive. We collimated the light source by passing it through a fiber-collimator, into a multimode optical fiber, and finally out from a second fiber-collimator.

The measurement proceeded as follows: We applied a 4 kHz square wave, amplitude-modulated with a linear ramp function with an envelope between $\sim 1.8 - 2.3$ V and a modulation frequency of 2 Hz. In this way, we were able to use an oscilloscope to capture the response of the photodiode. The measured photocurrent as a function of the applied voltage is shown in Fig. 6(b). We then utilized the calibration in Fig. 4(b) to convert from voltage to filter center wavelength, resulting in the data shown in Fig. 6(c) as the input to the reconstruction algorithm. The signal was then reconstructed using the deconvolution techniques outlined in Section 2.2 and the result is shown in Fig. 6(d).

The reconstructed spectrum has many of the features of the measured spectrum. Most prominently, the spectrum is low at the lower wavelengths and has a marked increase to brighter intensity at the higher wavelengths (both features roughly follow the test spectrum). As expected, the very sharp peak around 0.5 μm is not accurately reconstructed, but is smoothed out to a much lower and broader peak in the reconstruction. It is important to keep in mind that the $FWHM = 57$ nm for this particular test is substantially larger than the sharp peak (~ 10 nm), and yet the peak was not completely erased. Overall, we assert that the reconstructed spectrum is similar to that predicted by the discussion and equations in Section 2.2, and represents compelling evidence that the basic LCPG spectrophotometer concept is valid, and will be enhanced even further as the LCPG tunable filters improve.[15]

Several of the non-ideal characteristics of the reconstructed spectrum can be directly related to non-ideal features of the LCPG tunable filter. Most importantly, a noticeable amount of light leaks through our LCPG tunable filter in the upper stop-band (Fig. 4(a)), which clearly introduces a bias into the reconstruction process. A smaller distortion is due to the fact that the peak transmittance and FWHM of the filter are not constant with respect to voltage.[15] Finally, the FWHM of the LCPG filter used for this preliminary set of experiments is large (57 nm) compared to the features we wish to reconstruct (~ 10 nm), and will likely be significantly reduced by the addition of more and thicker LCPG stages in the filter. We believe that all of these effects are not a fundamental limitations to the LCPG filter, but rather are related to our (current) nascent skill at building them, and will be overcome as we fabricate better quality LCPGs at larger thicknesses.

6. CONCLUSION

We have experimentally demonstrated a compact spectrophotometer based on a polarization-independent LCPG tunable optical filter. The most critical aspects of our design include the absence of polarizers and the potential for very small size and low cost implementation. We derive the theoretical expressions which describe the system and the signal reconstruction process. We show both simulation and experimental results and conclude that they are well matched. The distortion in the reported proof-of-principle experiment reported here is directly linked to the not-yet ideal features of the tunable optical filter, and we anticipate a direct improvement in the function of the spectrophotometer as the LCPG filter technology[15] matures.
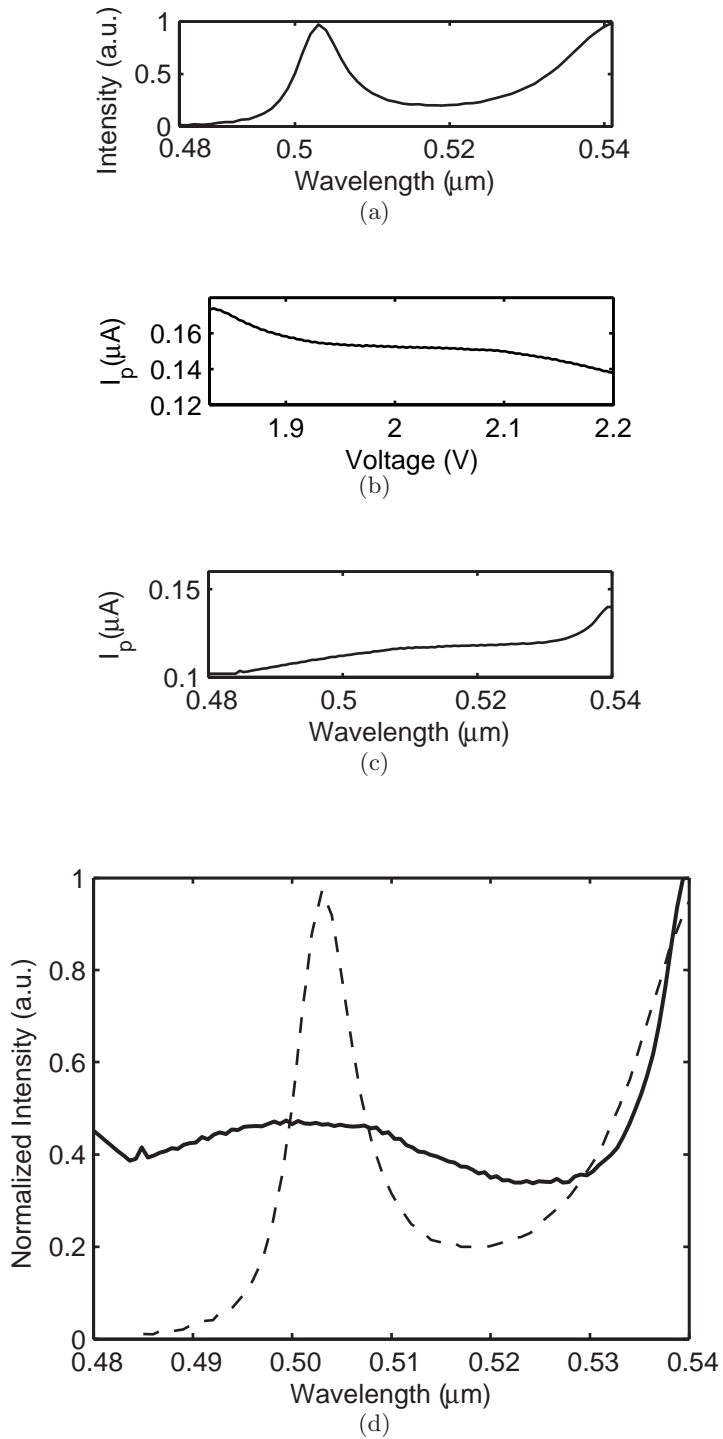
ACKNOWLEDGMENTS

Figure 6. Reconstruction by LCPG spectrophotometer: (a) Spectrum under test, created by passing white light from an incandescent lamp through an interference filter; (b) Measured photocurrent I_p as applied voltage is ramped linearly; (c) Measured I_p in terms of center wavelength of the tunable filter; and (d) Reconstructed spectrum.

REFERENCES

1. K. Rosfjord, R.A.Villalaz, and T. Gaylord, "Constant-bandwidth scanning of the Czerny Turner monochromator," *Applied optics* **39**(4), pp. 568–572, 2000.
2. A. Kenda, W. Scherf, R. Hauser, H. Gruger, and H. Schenk, "A compact spectrometer based on a micro-machined torsional mirror device," *Proceedings of IEEE Sensors* **3**, pp. 1312–1315, 2004.
3. A. Kutyrev, C.L.Bennett, S. Moseley, D. Rapchun, and K. Stewart, "Near infrared cryogenic tunable solid Fabry-Perot spectrometer," *Proceedings of SPIE* **5492**, pp. 1172–1179, 2004.
4. K. Hirabayashi and T. Kurokawa, "A tunable polarization-independent liquid crystal Fabry-Perot interferometer filter," *IEEE Photonics Technology Letters* **4**(7), pp. 740–742, 1992.
5. B.Lyot, "Filter monochromatique polarisane et ses applications en physique solarie," *Annales d'Astrophysique* **7**, p. 31, 1944.
6. H. Morris, C. Hoyt, P. Miller, and P. Treado, "Liquid crystal tunable filter raman chemical imaging," *Applied Spectroscopy* **50**(6), pp. 805–811, 1996.
7. A. Sneh and K. Johnson, "High-speed continuously tunable liquid crystal filter for WDM networks," *Journal of Lightwave Technology* **14**(6), pp. 1067–1080, 1996.
8. C. Ye, "Low-loss tunable filter based on optical rotatory dispersion," *Applied Optics* **45**(6), pp. 1162–1168, 2006.
9. I.Solc, "Birefringent chain filters," *Journal of the Optical Society of America* **55**(6), pp. 621–625, 1965.
10. B. Benkelfat, Q. Zout, and B. Vonouze, "Low-voltage continuous tunable hybrid filter for tailored optical-bandwidth operation," *IEEE Photonics Technology Letters* **16**(4), pp. 1098–1100, 2004.
11. J. Evans, "Solc birefringent filter," *Journal of the Optical Society of America* **48**(3), pp. 142–145, 1958.
12. J. Evans, "The birefringent filter," *Journal of the Optical Society of America* **39**(3), pp. 229–242, 1949.
13. C. Chen, C. Pan, C. Hsieh, Y. Lin, and R. Pan, "Liquid-crystal-based terahertz tunable Lyot filter," *Applied Physics Letters* **88**(10), pp. 101–107, 2006.
14. G. Keiser, *Optical Fiber Communications*, ch. 6, p. 246. McGraw-Hill, 3 ed., 2000.
15. E. Nicolescu and M. J. Escuti, "Polarization-independent tunable optical filters based on liquid crystal polarization gratings," *Proceedings of SPIE* **6654**, p. 4, 2007.
16. M. J. Escuti and W. M. Jones, "A polarization-independent liquid crystal spatial-light-modulator," *Proceedings of SPIE* **6332**, p. 633222, 2006.
17. W. M. Jones, B. L. Conover, and M. J. Escuti, "Evaluation of projection schemes for the liquid crystal polarization grating operating on unpolarized light," *SID Symposium Digest* **37**, pp. 1015–1018, 2006.
18. M. J. Escuti, C. Oh, C. Sanchez, C. W. M. Bastiaansen, and D. J. Broer, "Simplified spectropolarimetry using reactive mesogen polarization gratings," *Proceedings of SPIE* **6302**, p. 630207, 2006.
19. M. J. Escuti, C. Oh, C. van Heesch, C. Sanchez, C. W. M. Bastiaansen, and D. J. Broer, "Reactive mesogen polarization gratings with small pitch and ideal properties," *Advanced Materials* , p. submitted for publication, 2007.
20. G. Crawford, J. Eakin, M. Radcliffe, A. Callan-Jones, and R. Pelcovits, "Liquid-crystal diffraction gratings using polarization holography alignment techniques," *Journal of Applied Physics* **98**, p. 123102, 2005.
21. C. Provenzano, P. Pagliusi, and G. Cipparrone, "Highly efficient liquid crystal based diffraction grating induced by polarization holograms at the aligning surfaces," *Applied Physics Letters* **89**, p. 121105, 2006.
22. H. Sarkissian, S. V. Serak, N. Tabirian, L. B. Glebov, V. Rotar, and B. Y. Zeldovich, "Polarization-controlled switching between diffraction orders in transverse-periodically aligned nematic liquid crystals," *Optics Letters* **31**(15), pp. 2248–2250, 2006.
23. L. Nikolova and T. Todorov, "Diffraction efficiency and selectivity of polarization holographic recording," *Optica Acta* **31**, pp. 579–588, 1984.
24. J. Tervo and J. Turunen, "Paraxial-domain diffractive elements with 100% efficiency based on polarization gratings," *Optics Letters* **25**(11), pp. 785–786, 2000.
25. F. Gori, "Measuring stokes parameters by means of a polarization grating," *Optics Letters* **24**(9), pp. 584–586, 1999.
26. J. Eakin, Y. Xie, R. Pelcovits, M. D. Radcliffe, and G. Crawford, "Zero voltage Freedericksz transition in periodically aligned liquid crystals," *Applied Physics Letters* **85**(10), pp. 1671–1673, 2004.